Differentiation 148 (2026) 100947

Contents lists available at ScienceDirect

Differentiation

journal homepage: www.elsevier.com/locate/diff

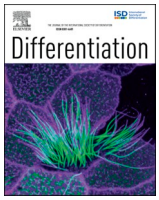

Ex vivo human cellular models to study adipocyte-induced transdifferentiation of osteoblasts

Federica Quacquarelli [a,*,1], Damien Leterme [a], Véronique Gauthier [a], Jérôme Delattre [a], Paiva dos Santos Bruno [a], Emeline Cailliau [b], Eric Fodzo [c], Antonella Poloni [d], Aline Clabaut [a], Odile Broux [a,**]

[a] Marrow Adiposity and Bone Laboratory - MABlab UR4490, Université du Littoral Côte d'Opale, F-62200 Boulogne sur Mer, Univ. Lille, F-59000 Lille, CHU Lille, F-59000, Lille, France
[b] Biostatistics Department, CHU Lille, F-59000, Lille, France
[c] Orthopedics and Traumatology Department, CH Boulogne-sur-mer, F-62200, Boulogne sur Mer, France
[d] Dipartimento Scienze Cliniche e Molecolari, Clinica di Ematologia, Università Politecnica delle Marche, Ancona, Italy

ARTICLE INFO

Keywords:
Human bone marrow stromal cells
Osteoblasts
Adipocytes
Transdifferentiation
Cellular models
Bone aging

ABSTRACT

In human, an association between bone loss and increased marrow adipose tissue suggests that medullary adipocytes could play a role in osteoporosis by acting on neighboring bone-forming osteoblasts. Supporting this hypothesis, we previously showed, using coculture and conditioned medium models based on human bone marrow stromal cells of commercial origin, that factors secreted by adipocytes induced the transdifferentiation of osteoblasts towards an adipocyte-like phenotype.

The aim of this study was to confirm the involvement of medullary adipocyte secretion products in the alteration of osteoblasts in pathophysiological conditions. To this end, two new cellular models were developed from human bone biopsies representing the aging skeleton. In the first model, outgrowth from trabecular bone fragments were used to isolate primary cells that displayed a specific osteoblast phenotype. We confirmed the transdifferentiation of these primary osteoblasts following their incubation with adipocyte conditioned medium as evidenced by the increase in the levels of adipogenic mRNA markers (PPARG, Leptin and HSD11B1, $P < 0,001$) and the decrease of osteogenic transcript (BGLAP, $P < 0.05$). The second model was based on primary adipocyte isolation through collagenase treatment followed by ceiling and 2D culture. Oil red O staining confirmed the isolation of fully-differentiated primary adipocytes from bone biopsies. Experiments performed with their conditioned medium validated what had been observed with primary osteoblasts: the effect of the adipocyte secretome on osteoblast fate. Overall, our results supported the relevance of these models to examine paracrine interactions between osteoblasts and adipocytes and confirmed the role played by adipocyte-secreted factors in osteoblast transdifferentiation.

1. Introduction

Maintenance of healthy bone mass requires a continuous process of bone remodeling, which consists of a balance of bone resorption by osteoclasts and bone formation by osteoblasts. With advancing age, an impairment of this balance leads to brittle bones and an increased risk of fractures, which represents the main hallmark of osteoporosis. A strong relationship between this bone loss and an increase in bone marrow adipose tissue suggests a potential role for medullary adipocytes in the deficiency of osteoblasts to replace the resorpted bone (Hardouin et al., 2014; Meunier et al., 1971; Rosen and Bouxsein, 2006). This hypothesis is supported by the proximity of adipocytes to osteoblasts, their shared multipotent precursor, the bone marrow stromal cell (BMSC), and the fact that adipocytes are secretory cells (Muruganandan et al., 2018; Sadie-Van Gijsen et al., 2013). In an attempt to reproduce cellular interactions within the bone marrow, we previously developed cellular

* Corresponding author.
** Corresponding author.
E-mail addresses: federica.quacquarelli@bme.lth.se (F. Quacquarelli), odile.broux@univ-littoral.fr (O. Broux).
[1] Present address Department of Biomedical Engineering, Lund University, Lund, Sweden.

https://doi.org/10.1016/j.diff.2026.100947
Received 4 September 2025; Received in revised form 5 February 2026; Accepted 6 February 2026
Available online 7 February 2026

models using human BMSC-derived osteoblasts and adipocytes. With these models, we demonstrated that soluble factors secreted by adipocytes induced the conversion of osteoblasts towards an adipocyte-like phenotype (Clabaut et al., 2010). This change in fate was further confirmed by double immunofluorescence staining that demonstrated the co-expression of adipogenic and osteoblast specific markers at the single cell level providing evidence for a transdifferentiation event. Complementary to these *in vitro* results, preliminary immunohistochemical analysis revealed adipogenic marker expression in osteoblasts from elderly subjects, suggesting that osteoblast transdifferentiation could contribute to decreased bone mass in aging (Clabaut et al., 2021).

In this study, our aim was to confirm the involvement of medullary adipocyte secretion products in the alteration of osteoblasts in pathophysiological conditions. To this end, two new cellular models were developed from human bone biopsies representing the aging skeleton. We used human femoral heads to establish (1) an outgrowth model based on the spontaneous migration of human osteoblast-like cells (hOB) using the explant technique (Dillon et al., 2012; Gartland et al., 2012) (2) a model based on primary adipocytes isolated through collagenase treatment followed by ceiling and adherent culture (Mattiucci et al., 2018). In both models, we investigated the osteoblastic response to secreted factors released from medullary adipocytes using conditioned media incubations. Phenotypic changes in osteoblastic cells were determined by analyzing their gene expression profiles and comparing them with those of non-incubated controls. In the first model, phenotype variations were eventually related to bone density and microarchitecture data determined by X-ray microtomography (μCT) to assess the existence of a correlation between the osteoblast response to adipocyte secretions and the quality of the bone from which the cells were derived.

2. Materials and methods

2.1. Human clinical sample acquisition

Femoral heads used for the first model were obtained from twenty patients undergoing total hip replacement in the department of Traumatology at Boulogne-sur-mer hospital, France. Specimen were collected from 13 female and 7 male patients (median age 72, range 52-92). The study procedures were approved by the local Institutional Review Board (2020-A00027-32), and complied with the ethical standards of the relevant institutional and national Human Experimentation Ethics Committees (reference CPP 20/18). The seven femoral heads used for the second model were obtained from 5 female and 2 male patients (median age 71, range 48-89) in the Orthopedic department of the Riuniti di Torrette hospital in Ancona, Italia. Tissue samples were collected in accordance with local ethics committee guidelines (300/DG) and written informed consent was obtained from all participants. Patients with bone diseases other than osteoarthritis or osteoporosis, or suffering from cancer, were excluded from the study.

2.2. Cell culture experiments

2.2.1. Isolation and culture of human osteoblast-like cells

Following surgery, discarded femoral head specimen was cut longitudinally into 2 parts and placed on ice in sterile phosphate-buffered saline (PBS) supplemented with 1% penicillin/streptomycin/amphotericin (Pan Biotech, Dutscher, France). One half of the biopsy was used immediately for cell culture experiments, the other half was frozen at −20 °C until μCT analyses.

Trabecular bone fragments up to 5 mm were initially extracted from the central part of the femoral head, thus avoiding subchondral regions. Some explants were reserved for histological analyses, the other were placed in a petri dish containing sterile PBS, divided into pieces approximately 3-5 mm in diameter and thoroughly rinsed in PBS. The fragments were placed in 100-mm diameter culture dishes (around 20 fragments per dish) and covered with expansion medium composed of Dulbecco's Modified Eagle Medium (DMEM) (Pan Biotech, Dutscher, France) containing 10% fetal calf serum (FCS), 1% penicillin/streptomycin and 1% glutamine (Pan Biotech, Dutscher, France). Dishes were incubated at 37 °C in a humidified atmosphere of 95% air and 5% CO_2 and were left undisturbed for 6 days, then the medium was changed every two days. At day 10, the bone fragments were removed from the culture dish, cut again to stimulate fresh cell outgrowth and placed in a six well plate with an average of 6 to 8 fragments per well. The fragments were cultured in expansion medium with osteogenic inducers (50 mM ascorbic acid, 10 mM β-glycerophosphate and 10^{-8} M vitamin D3) (Sigma-Aldrich, France) until the full confluence was achieved (approximately three weeks).

2.2.2. Alizarin red staining

The mineralization was investigated by alizarin red staining. Briefly, cells were fixed in 2% paraformaldehyde for 15 min, rinsed and stained with 2% Alizarin red solution (Sigma Aldrich, France) for 30 min at room temperature. Excess dye was removed by washing with distilled water.

2.2.3. Isolation and culture of human bone marrow primary adipocytes

Bone marrow adipocytes were isolated according to a method previously described, with validation of primary adipocyte purity through microarray analysis (Mattiucci et al., 2018). Briefly, the femoral heads were cut into four parts and incubated at 37 °C for 90 min in agitation in a solution containing 1 mg/ml of type I collagenase (Sigma-Aldrich). Supernatants were then filtered, washed four times with DMEM and centrifuged at 250g for 5 min. Collection of the upper layer after each centrifugation provided floating adipocytes which were seeded for ceiling culture in flask filled to capacity with 10% FCS DMEM incubated upside down and placed at 37 °C in a humidified atmosphere of 95% air and 5% CO_2. Three days later, the medium was removed, the flask was inverted and the cells were then cultured in classical orientation in expansion medium supplemented with adipogenic inducers (0.5 μM dexamethasone, 0.5 mM isobutyl-1-methylxanthine and 50 μM indomethacin (Sigma-Aldrich)) (Laharrague and Casteilla, 2007) during one week with two changes of media.

2.2.4. Oil red O (ORO) staining

Isolated adipocytes were fixed in 2% paraformaldehyde for 15 min, rinsed with water, incubated with 60% isopropanol for 5 min and stained with newly filtered ORO solution for 10 min at room temperature. After staining, the cells were rinsed with water before counterstaining with Haematoxilin solution for 5 min at room temperature.

2.2.5. Human bone marrow stromal cell culture and differentiation

Human bone marrow stromal cells (hBMSCs, Rosterbio, USA) at passage 4 to 8 were plated in 6-well plates in expansion medium. Cell cultures were maintained at 37 °C in a humidified atmosphere of 95% air and 5% CO_2, and the media were changed twice weekly. Differentiation experiments were started when hBMSCs had reached confluence (day 0). To induce osteogenesis, hBMSCs were cultured in expansion medium supplemented with osteogenic inducers for 14 days. For adipogenic differentiation, hBMSCs were cultured in expansion medium supplemented with adipogenic inducers for 10 or 14 days. The differentiation protocols were previously validated by using real-time PCR (Clabaut et al., 2015; Martin et al., 2015).

2.2.6. Conditioned medium experiments: first cellular model

On day 10 of differentiation, hBMSC-derived adipocytes were placed in serum-free DMEM for 48 h. The supernatants were then collected and applied to primary cultures of human osteoblast-like cells (hOB). Osteoblasts were incubated in conditioned medium for 48 h. As controls, osteoblasts were incubated with serum-free DMEM for the same time. Cells were then lysed for RNA extraction.

2.2.7. Conditioned medium experiments: second cellular model

After a week of regular culture, primary adipocytes were cultured in serum and inducer-free DMEM for two days. The supernatants were collected and used to incubate hBMSC-derived osteoblasts (hBMSC-OB) at day 12 of differentiation for 48h. hBMSC-OB incubated in serum free DMEM were used as controls.

2.3. Characterization of bone fragments

2.3.1. Paraformaldehyde inclusion

Bone explants were fixed in 10% buffered formalin for 48 h at 4 °C. The fragments were then washed with PBS and decalcified in 12,5% EDTA/NaOH at pH7 for 2 weeks at 4 °C, with solution change every three days. After three washes in PBS, the explants were embedded in paraffin and sectioned at 6-8 μm thickness using microtome RM2255, Leica. Tissue sections were stained with Haematoxilin-Eosin (H&E) or processed for immunohistochemical analysis.

2.3.2. H&E staining

Sections were deparaffinized in xylene and rehydrated in graded ethanol before staining with H&E. Three sections were evaluated throughout the biopsy every 60 μm of intervals.

2.3.3. Immunohistochemistry

Deparaffinized and rehydrated sections were subjected to antigen retrieval with citrate buffer for 1h at 65 °C, permeabilization with Triton X 0,1% in PBS for 10 min and treatment with 3% hydrogen peroxide to inactivate endogenous peroxidase. After blocking with 1% bovine serum albumin, sections were incubated overnight at 4 °C with anti-BGLAP antibody (Abcam ab198228, 1:400) and, after PBS washes, incubated 1 h with biotin-conjugated secondary antibody (Dako E0432, 1:1000). Detection was done by incubation with Streptavidin/HRP (Dako P0397, 1:800) and Diamino-benzedine (Sigma D4293). Sections were counter-stained with Haematoxilin and mounted using Eukitt solution.

2.4. RNA expression measurement

2.4.1. RNA isolation

Total RNA was extracted using the RNeasy® Micro Kit, including the DNase I digestion step (Qiagen, France), according to the manufacturer's instructions and quantified by Nanodrop at the wavelength of 260 nm.

2.4.2. mRNA expression analysis

Total RNA was reverse transcribed using Maxima First-Strand cDNA Synthesis kit (Fermentas, Thermoscientific, France), and subjected to quantitative real-time PCR on the LightCycler® Carousel-Based System (Roche Diagnostics, France) using the LightCycler® Fast Start DNA Master SYBR® Green I kit and specific primers designed using Oligo 6 software (MedProbe, Norway) (Table 1). Relative gene expression levels were normalized to YWHAZ (tyrosine 3-monooxygenase/tryptophan 5-monooxygenase activation protein), and PPIA (peptidylprolyl isomerase A) transcripts and determined using the $2^{-\Delta\Delta Ct}$ method.

2.5. X-ray microtomography(μCT)

Two to three cylindrical trabecular bone samples were harvested from frozen human biopsies using a 9 mm diameter hole-saw. Samples were fixed in 10% formalin for 72 h at 4 °C, then kept in ethanol 70% until processed. Each explant was scanned by microtomography (Skyscan 1172, Bruker) with the following parameters: 100 kV, 100 μA, AL + Cu filter, 2200 ms as exposure time, 0.3 rotation step over 180°, frame averaging 3, pixel size 10 μm and a field of view 2000 px by 1332 px. The following parameters were setting to rebuild acquisition dataset with NRecon software (Bruker), according to manufacturer's protocol: ring artefact reduction 3, beam hardening compensation 20%, smoothing 2.

Image grey levels range was standardized for the whole study to guarantee the same grey levels throughout all reconstructed datasets. The analysis was done with the CTan software (Bruker), according to a volume of interest of 400 mm3 with a cylinder of diameter 9 mm. The multi-level Otsu was used for binarization.

The trabecular bone microarchitectural parameters chosen for evaluation were bone volume fraction (BV/TV), bone surface fraction (BS/TV), trabecular number (Tb.N), trabecular thickness (Tb.Th), trabecular spacing (Tb.Sp) and trabecular pattern factor (Tb.Pf).

Table 1
Primer sequences.

cDNA	Forward and reverse primers	Product (bp)	Genbank
BGLAP	F:5′- ATGAGAGCCCTCACACTCCTC -3′ R:5′- GCCGTAGAAGCGCCGATAGGC -3′	293	NM_199173
HSD11B1	F:5′- CAGCAAAGGGATCGGAAGA -3′ R:5′- AAATTGCTCTGCGAAGGTCA -3′	181	NM_005525
LEP	F:5′- ATTTCACACACGCAGTCAGT -3′ R:5′- GAAGAAGATCCCGGAGGT -3′	262	NM_000230
PPARG	F:5′-GCTTCTGGATTTCACTATGG-3′ R:5′-AAACCTGATGGCATTATGAG-3′	195	NM_015869
PPIA	F:5′-ACCGTGTTCTTCGACATTGC-3′ R:5′-CAGGACCCGTATGCTTTAGGA-3′	274	NM_021130
YWHAZ	F:5′-GGTCATCTTGGAGGGTCGTC-3′ R:5′-GTCATCACCAGCGGCAAC-3′	245	NM_145690

Shown are the primer sequences, lengths of the corresponding PCR products, and Genbank accession numbers. F: forward; R: reverse. BGLAP, Bone Gamma-Carboxyglutamate Protein; HSD11B1, hydroxysteroid (11-beta) dehydrogenase 1; LEP, Leptin; PPARG, peroxisome proliferator-activated receptor gamma; PPIA, peptidylprolyl isomerase A; YWHAZ, tyrosine 3-monooxygenase/tryptophan 5-monooxygenase activation protein.

2.6. Statistical analysis

Statistical significance of mRNA level relative variations was evaluated for each gene using Wilcoxon's signed rank test. Associations between patient age and μCT data and associations between the response of hOB to adipocyte secretions and μCT data were evaluated using Spearman correlation coefficients.

3. Results

3.1. Experimental study design and workflow

In the first model, trabecular bone fragments harvested from human bone biopsies were used to isolate osteoblast-like cells (hOB) according to a method adapted from Dillon et al. (2012). Briefly, this explant culture method relied on cellular outgrowth of cells from explants in two consecutives phases, first and second migration. The effects of adipocyte secretome on primary cells from the second migration were analyzed after their incubation in conditioned medium provided by BMSC-derived adipocytes of commercial origin. The use of BMSC-derived cells was introduced to normalize the variability among the different donors. Phenotypic changes in osteoblastic cells were determined by analyzing their gene expression profiles and comparing them with those of non-incubated osteoblasts. Gene expression results were finally correlated with bone microarchitecture data obtained on explants using μCT analyses (Fig. 1A). The second model was developed to investigate the effect of primary adipocyte secretome on BMSC-derived osteoblasts. Primary bone marrow adipocytes were isolated from femoral heads using enzymatic digestion followed by washing steps. Cells were then cultured first using the ceiling method then in normal 2D culture until their media were collected and used to incubate hBMSC-OB for 48 h. Osteoblasts were then lysed for RNA extraction and gene expression analyses were performed (Fig. 1B). These two models were thus inverted: both examined the influence of the

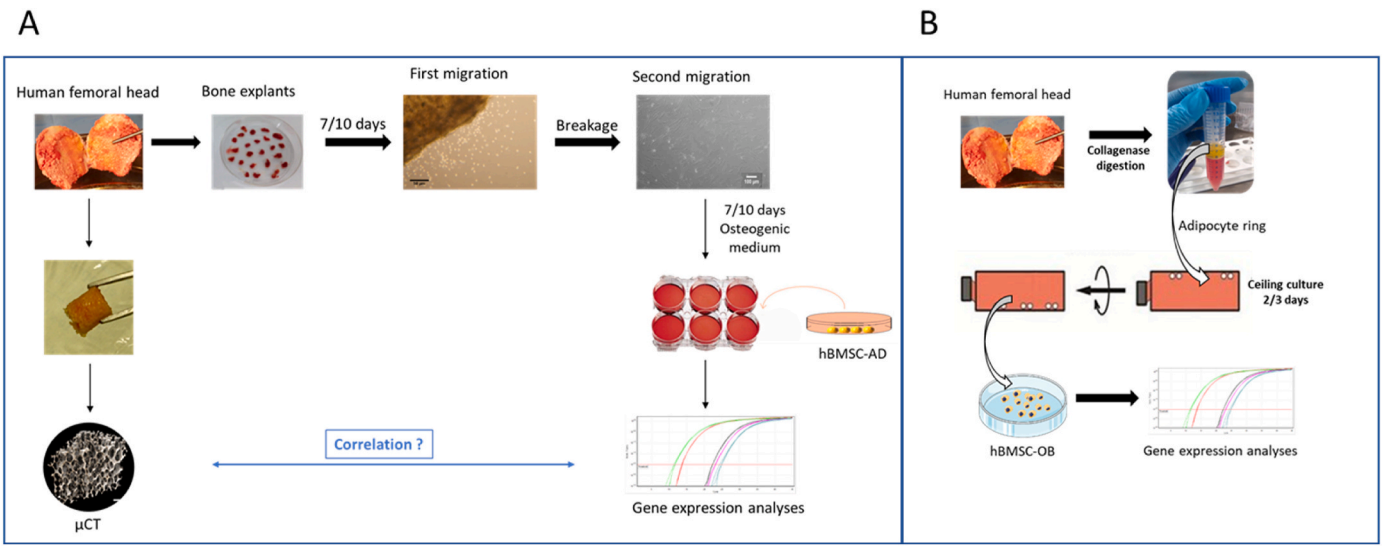

Fig. 1. Experimental workflow A. Human osteoblast-like cells were isolated from femoral head following two rounds of migration. Cells of the second migration were incubated in conditioned medium from human bone marrow stromal-derived adipocytes of commercial origin (hBMSC-AD). Gene expression changes in the osteoblastic population were then analyzed by using real-time reverse transcription polymerase chain reaction. Phenotype variations were finally correlated with bone microarchitecture data obtained on explants using µCT analyses. B. Primary bone marrow adipocytes were isolated from human femoral head using collagenase digestion. Cells were cultured using the ceiling method then in normal 2D culture until their media were collected and used to incubate human bone marrow stromal-derived osteoblasts of commercial origin (hBMSC-OB). Gene expression changes in the osteoblastic population were then analyzed by using real-time reverse transcription polymerase chain reaction.

adipocyte-conditioned medium on osteoblast differentiation, but the primary and BMSC-derived cells were swapped in model 1 compared to model 2.

3.2. Development of the outgrowth model using the explant technique

3.2.1. Characterization of bone fragments

Bone samples were obtained from patients undergoing total hip replacement, mainly because of coxarthrosis. Osteoarthritis is defined as a disease of the articular cartilage and subchondral bone. We only sampled trabecular bone fragments of the central part of the femoral head, thus avoiding subchondral regions. To confirm that normal trabecular bone has been collected, histological analyses were performed. H&E staining revealed typical mineralized and marrow compartment histology (Fig. 2A). Bone trabeculae presented osteocytes in lacunae and osteoblasts along the bone lining and the marrow cavity was filled with hematopoietic cells and adipocytes. In addition, BGLAP (Bone Gamma-Carboxyglutamate Protein, alias Osteocalcin) immunoreactivity was seen in some osteocytes and in lining osteoblasts at the surface of the trabecular bone (Fig. 2B), confirming the presence of functional bone cells in the samples.

3.2.2. Isolation and culture of hOB

We based our approach on that of Dillon et al. (2012) to isolate primary hOB. This 2D model was built on the spontaneous outgrowth of cells from the bone explant. The first signs of cell migration from explants were observed within 5-10 days of plating. The cell population was heterogeneous (Fig. 3A), including fibroblast-like cells, hematopoietic cells and adherent non-stem cells with different proportions depending on the donor. According to alizarin staining, cells were not able to deposit mineralized matrix (data not shown), hinting the lack of mature osteoblasts or their minor presence in the population. At this stage, by cutting again the fragments to stimulate the growth of new cells, a second migration was initiated. Cells began to migrate 4-5 days after the second cut, and full confluence was generally reached after 3 weeks.

To encourage osteoblast migration, the fragments were cultured in osteogenic medium. Cell population was more homogenous, showed characteristic cell morphology and formed a continuous layer of tissue (Fig. 3B). Alizarin red staining was able to detect matrix mineralization in some cultures (Fig. 3C), but not in all, revealing inter-donor variability. Quantitative RT-PCR results showed that the cells expressed ALPL and RUNX2 at levels comparable to those of hBMSC-OB cells (Fig. 3D). In addition, late osteoblastic differentiation was evidenced by the expression of BGLAP with mRNA levels significantly higher than in hBMSC-OB ($P < 0.05$) (Fig. 3D).

3.2.3. Conditioned medium experiments

The conditioned medium experiments were carried out on the cell population from the second migration, which was more homogeneous than the one from the first migration. The effect of adipocyte secretome on hOB was analyzed after their incubation for 48h in conditioned medium provided by BMSC-derived adipocytes of commercial origin. The gene expression analysis showed that the mRNA levels of adipocyte genes were significantly upregulated in hOB after the treatment compared to the control in serum-free DMEM (Fig. 4). In addition, quantitative RT-PCR results highlighted a significant decrease of BGLAP and SPP1 mRNA levels in hOB following incubation in adipocyte-conditioned medium (Fig. 4). Compared to hBMSC-OBs, hOBs exhibited similar variations in gene expression levels in response to incubation in conditioned medium (Fig. 5).

3.2.4. µCT analyses

Using calibrated trabecular bone samples from femoral heads, µCT was performed to determine morphometric parameters of bone biopsies. The values obtained were compared with data derived from healthy and osteoporotic bones found in the literature (Chappard, 2012). Some samples displayed values comparable to those of osteoporotic bone, in particular two biopsies from patients undergoing surgery for femoral neck fractures (Table 2). This confirms the validity of the method used, with µCT data providing valuable insights into the bone quality of patients' femoral heads (Fig. 6). Supporting this, the patient's age was positively correlated with Trabecular Spacing (Tb.Sp) parameter ($\rho = 0.45$ $p = 0.046$), consistent with the age-related impact on trabecular bone microarchitecture. It also appeared a negative correlation with the number of trabeculae (Tb.N) and the percentage of bone volume

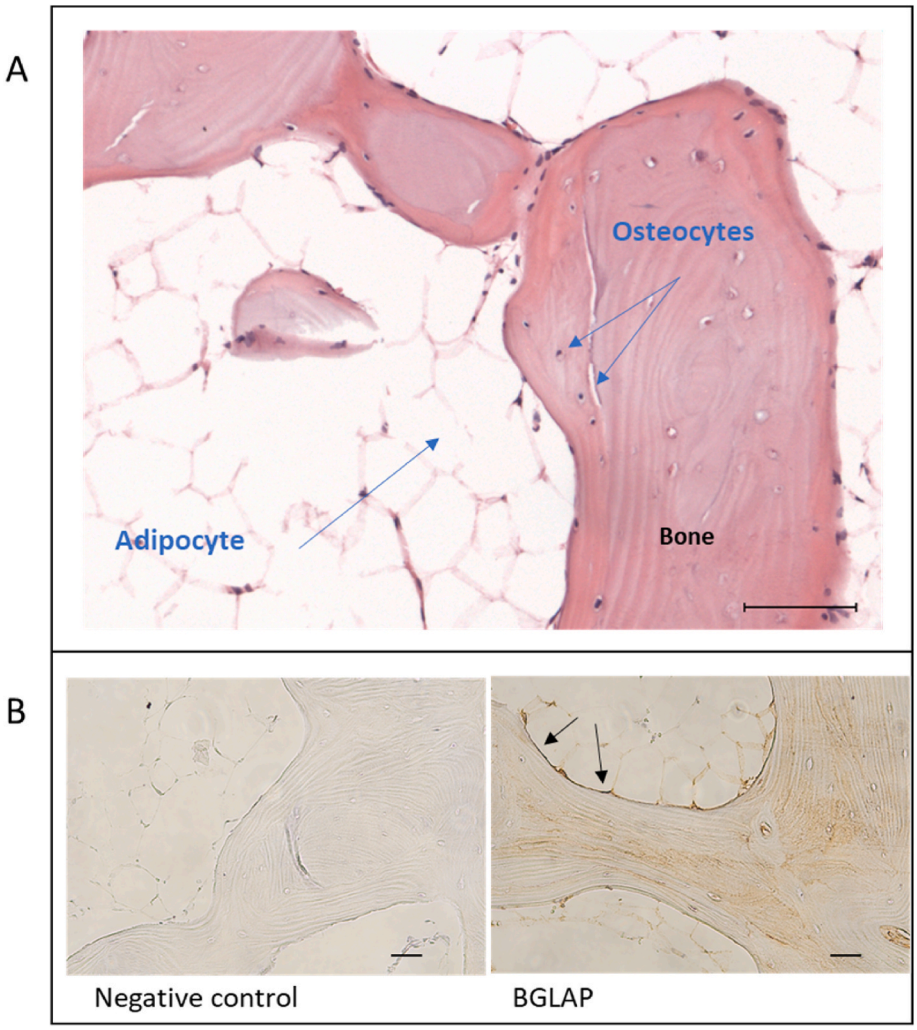

Fig. 2. Characterization of bone fragments A. Representative H&E stained section of bone fragment showing abundant adipocytes in the bone marrow next to mineralized bone with osteocytes. Bar = 100 μm. B. Representative histological slides of BGLAP (Bone Gamma-Carboxyglutamate Protein) immunoreactivity in human bone samples. The black arrows point out the presence of lining osteoblasts expressing BGLAP. Bar = 50 μm.

(BV/TV), but without reaching statistical significance ($\rho = -0.42$ and $p = 0.063$ and, $\rho = -0.42$ and $p = 0.083$, respectively). One of the aims of this study was to assess whether or not there was a correlation between the response of hOB to adipocyte secretions and the quality of the subject's bone tissue from which these osteoblasts originated. However, statistical analyses did not reveal any significant association between gene expression changes in hOB incubated in conditioned medium and μCT parameters (Supplementary Table 1).

3.3. Preparation and use of primary adipocyte secretome

Primary adipocytes isolated from bone biopsies were first cultured using the ceiling method. The Oil red O staining confirmed the presence of fully mature and rich-in-lipid adipocytes (Fig. 7A). Ceiling culture enables the floating adipocytes to adhere to the inner top surface of a flask fulfilled with medium. However, it has been shown that adhered cells rapidly dedifferentiate into fibroblast-like cells (Poloni et al., 2015). That's why, after two to three days of ceiling culture, the cells were cultured in classical orientation in expansion medium supplemented with adipogenic inducers during one week. Primary adipocytes were then cultured in serum and inducer-free DMEM for two days before their media were used to incubate hBMSC-OB. The gene expression analysis pointed out an increase in the mRNA levels of adipogenic genes, particularly PPARG, as well as a decrease in the BGLAP mRNA levels (Fig. 7B).

Similar gene expression variations, obtained using the conditioned medium collected at the end of the ceiling culture, ruled out the potential involvement of inductors in these phenotypic modifications and further strengthened these results. (Supplementary Fig. 1).

4. Discussion

The aim of this study was to develop new cellular models to confirm the osteoblast response to adipocyte secretome in a more relevant representation of the human bone environment in pathophysiological conditions. For this, we chose to use primary cells derived from human bone biopsies representing the aging skeleton. The majority of the donors were suffering for osteoarthritis (OA), the others from osteoporosis (OP). Both OP and OA affect elderly people. While OP is marked by a decrease of bone density and microarchitectural disruption, OA is considered a disease of the articular cartilage and the subchondral bone. Despite their relationship is still not clarified, clinical evidences pointed out a possible comorbidity between OP and OA (Geusens and van den Bergh, 2016; Rizou et al., 2018). *In vitro* studies identified differences in primary cell behaviour that are linked to their anatomical location in bone (Shah et al., 2015). To prevent this, all the bone fragments were extracted from the central trabecular part of the femoral head, thus avoiding subchondral regions which play a crucial role in the

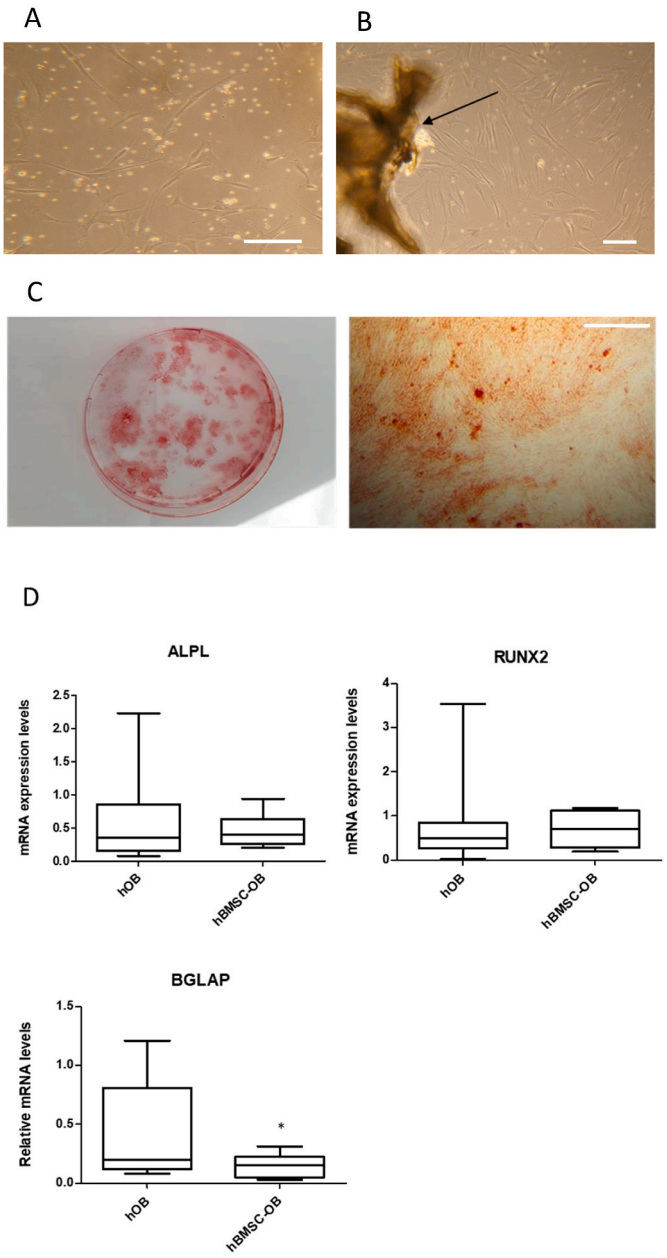

Fig. 3. Isolation and culture of hOB A. Representative phase contrast picture of cell population ten days after setting up the culture. Bar = 100 μm. B. Representative phase contrast picture of second cellular outgrowth after 10 days of culture in osteogenic medium. The black arrow points to a bone fragment. Bar = 100 μm. C. Mineralization assay on hOB. The alizarin Red staining is visible at macro level and at cellular level. Bar = 100 μm. D. Comparison of ALPL (Alkaline Phosphatase), RUNX2 (RUNX Family Transcription Factor 2) and BGLAP (Bone Gamma-Carboxyglutamate Protein) mRNA levels in Osteoblast-like cells (hOB) and hBMSC-derived osteoblasts (hBMSC-OB). Quantitative RT-PCR analysis was performed when full confluence was achieved, that is, approximately 2 or 3 weeks after the onset of osteogenesis for hBMSC-OB and hOB, respectively. mRNA expression levels were normalized against the signal from two housekeeping genes for peptidylprolyl isomerase A (PPIA) and tyrosine 3-monooxygenase/tryptophan 5-monooxygenase activation protein (YWHAZ). Results are presented as the median and 1st and 3rd quartile. N = 20 for each group. *P < 0.05 for hBMSC-OB compared to hOB.

pathophysiology of OA. Despite this precaution, the primary cells display inherent variability amongst donors. The use of BMSC-derived cells, as adipocytes in the first model and as osteoblasts in the second one, was therefore introduced for standardization purposes.

Primary osteoblasts are usually isolated from bone using collagenase digestion or explant culture method. Advantages of the explant method include absence of proteolytic stress and presence of the tissue pieces, providing extracellular matrix signals, proteins and growth factors (Hendijani, 2017). We decided to adopt the protocol described by Dillon (Dillon et al., 2012) with some minor changes. The functional assay and the gene expression results confirmed the effective osteoblastic nature of those cells and, thus, the reliability of the method. Not only the isolated cells were osteoblasts, but their expression levels of osteogenic markers, particularly BGLAP, were higher than the ones expressed by BMSC-derived osteoblasts. Incubation experiments with adipocyte conditioned medium gave results similar to those obtained with BMSC-derived osteoblasts of commercial origin (Clabaut et al., 2010, 2021): the appearance of a hybrid phenotype, with the expression of both lineage markers but without the conversion into mature adipocytes, indicative of a partial transdifferentiation event.

Experiments performed with conditioned medium from primary adipocytes confirmed what had been observed with primary osteoblasts: the effect of the adipocyte secretome on osteoblast fate. A limitation of the earlier experiments was the use of conditioned medium derived from adipocytes cultured in the presence of adipogenic inducers. Although the cells were subsequently incubated for at least two days without serum and inducers, the potential presence of residual inducers, capable of affecting osteoblast behaviour, cannot be totally ruled out. However, the use of adipogenic inducers remains necessary in primary adipocyte cultures due to their tendency to dedifferentiate (Poloni et al., 2015). An experiment using conditioned medium from the ceiling culture was therefore carried out to clarify this point. Ceiling culture was performed for two to three days after cell recovery, in complete medium without inducer. These cells are therefore representative of adipocytes in their physiological environment. The fact that their conditioned medium had an effect on osteoblasts reinforces that factors secreted by the adipocytes themselves are responsible for this phenomenon, and rules out a bias due to culture.

Transdifferentiation, also known as lineage reprogramming, is the conversion of one mature somatic cell into another cell type without going through a pluripotent state (Merrell and Stanger, 2016). This phenotype switch has already been observed between osteogenic cells and adipocytes in various cell culture models in response to inductive media or even physical factors such as microgravity (Nuttall et al., 1998; Schilling et al., 2007; Song and Tuan, 2004; Zhang et al., 2018). Compared with these studies, the osteoblastic transdifferentiation observed in our models is not due to an external factor but to the paracrine effect of adipocyte secretions. To identify adipocyte-secreted factor(s) causing a shift of osteoblasts towards an adipocyte-like phenotype, we previously used an integrative Omics strategy combining proteomic and transcriptomic data from both cell types. This approach allowed us to propose three pathways potentially involved in the osteoblast transdifferentiation: The PI3K-AKT (phosphatidylinositol 3-kinase- protein kinase B) pathway and the JAK2-STAT3 (Janus kinase 2/signal transducers and activators of transcription 3) pathway could promote adipogenesis following the binding of IGF2 (Insulin-like Growth Factor 2), ANGPT4 (Angiopoietin 4) or LEP (Leptin) to their respective receptor. On the other side, the inactivation of the SMAD pathway through the presence in the adipocyte secretome of inhibitors of BMP (Bone Morphogenic Protein), TGFBB (Transforming Growth Factor Beta) and Activin signaling could repress osteogenesis (Salmi et al., 2022).

This transdifferentiation could contribute to the increase in bone marrow adipose tissue at the expense of osteoblast number, and therefore play a role in the decrease in bone formation. We thus investigated whether there was a correlation between the response of osteoblasts to adipocyte secretions and the microarchitectural quality of the bone tissue used for cell isolation. X-ray microtomography (μCT) is a tool widely used to evaluate three-dimensional structure data of bone tissue. With that technique, it is possible to evaluate bone microarchitecture

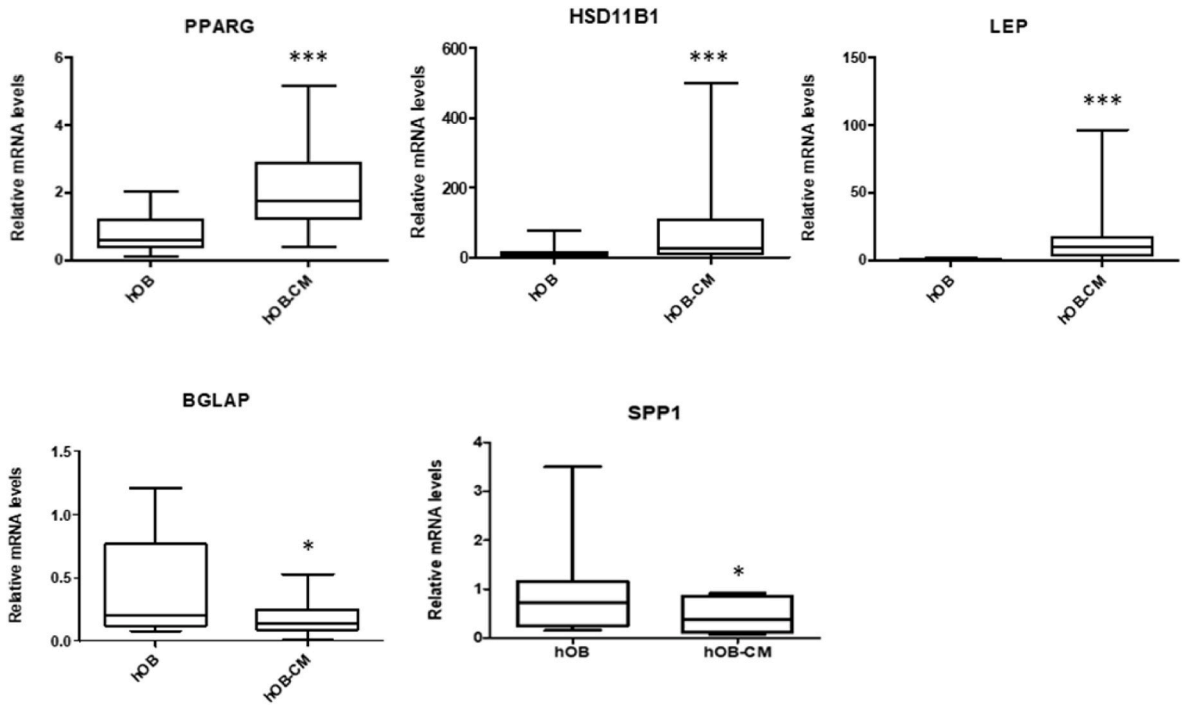

Fig. 4. Effect of adipocyte secretome on hOB
Quantitative RT-PCR analysis of adipocyte-specific genes, PPARG (Peroxisome proliferator-activated receptor gamma), HSD11B1 (Hydroxysteroid (11-beta) dehydrogenase 1), LEP (Leptin) and osteoblast-specific genes BGLAP (Bone Gamma-Carboxyglutamate Protein) and SPP1 (Secreted phosphoprotein 1). hOB: Osteoblast-like cells in serum free medium for 48 h hOB-CM: hOB incubated for 48h in conditioned medium provided by BMSC-derived adipocytes. mRNA expression levels were normalized against the signal from two housekeeping genes for peptidylprolyl isomerase A (PPIA) and tyrosine 3-monooxygenase/tryptophan 5-monooxygenase activation protein (YWHAZ). Results are presented as the median and 1st and 3rd quartile. N = 20 for each group. *P < 0.05, ***P < 0,001 for hOB-CM compared to hOB.

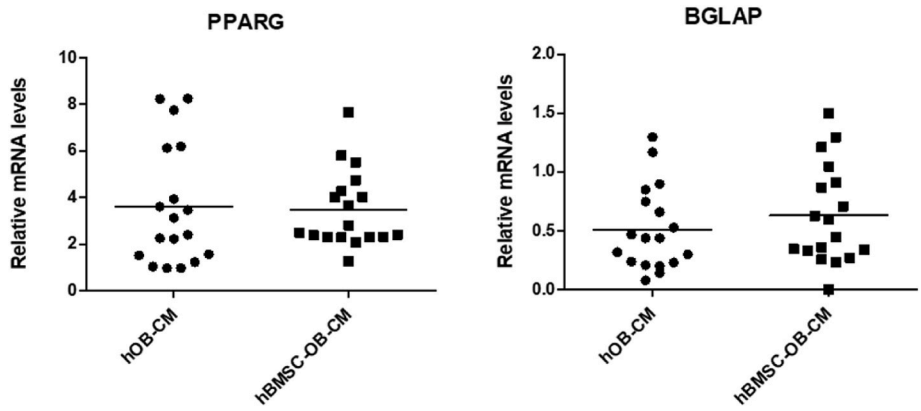

Fig. 5. Comparison of response to the conditioned medium between hOB and hBMSC-OB
Quantitative RT-PCR analysis of adipocyte-specific gene, PPARG (Peroxisome proliferator-activated receptor gamma), and osteoblast-specific gene BGLAP (Bone Gamma-Carboxyglutamate Protein). hOB-CM: Osteoblast-like cells incubated for 48h in conditioned medium provided by BMSC-derived adipocytes. hBMSC-OB-CM: hBMSC-derived osteoblasts incubated for 48h in conditioned medium provided by BMSC-derived adipocytes. mRNA expression levels were normalized to non-incubated control cells against the signal from two housekeeping genes for peptidylprolyl isomerase A (PPIA) and tyrosine 3-monooxygenase/tryptophan 5-monooxygenase activation protein (YWHAZ). N = 19 for each group.

changes in relation to mechanical stress, effects of age, osteoporosis or anti-osteoporotic drugs (Effendy et al., 2013; Ravazzano et al., 2024). Our data revealed a positive correlation between patient age and trabecular spacing parameter, as previously reported in the trabecular bone of the femoral head (Chen et al., 2013). On the other hand, statistical analyses did not reveal any significant association between gene expression changes in primary osteoblasts incubated in conditioned medium and μCT parameters. This result could be explained by the small sample size in our study (n = 20) as well as variations within the osteoblastic population in terms of basal gene expression levels and response to adipocyte secretions.

In summary, the new models based on primary cells isolated from bone biopsies have confirmed the role played by adipocyte-secreted factors in the transdifferentiation of osteoblasts. This phenomenon could explain the link between bone loss and accumulation of medullary adipocytes in conditions such as aging and osteoporosis and could participate, at the local level, in age-related bone loss. In the course of our experimental efforts to decipher the mechanisms of this

Table 2
Bone histomorphometric parameters of trabecular bone samples determined by µCT.

Age/Gender patients	BV/TV	BS/TV	Tb.Th	Tb.N	Tb.Sp	Tb.Pf
75/F	25.06	6.21	0.14	1.80	0.88	-2.83
57/F	19.49	4.40	0.16	1.24	0.67	1.93
72/F	25.33	6.26	0.14	1.85	0.56	-2.63
82/F	14.96	3.08	0.17	0.88	1.07	-3.08
53/F	19.37	4.41	0.15	1.26	0.68	0.41
92/F	10.49	3.09	0.12	0.84	0.78	5.91
57/F	22.95	5.46	0.14	1.61	0.56	-1.84
80/M	13.54	3.65	0.13	1.05	0.74	4.16
72/M	20.62	3.73	0.19	1.08	0.71	3.47
76/F	14.80	2.57	0.20	0.72	1.01	3.87
90/F	17.43	3.25	0.19	0.91	0.85	3.33
73/F	21.81	3.99	0.19	1.13	0.65	2.70
52/M	29.84	5.81	0.17	1.72	0.48	0.53
74/M	27.55	4.59	0.20	1.36	0.61	0.91
68/M	31.76	5.37	0.20	1.60	0.57	0.56
74/F	33.17	5.47	0.20	1.61	0.50	1.55
66/F	37.32	4.56	0.27	1.35	0.64	0.39
81/M	24.96	5.13	0.16	1.56	0.63	1.97
61/M	17.80	3.67	0.17	1.02	0.73	3.96
80/F	29.64	4.83	0.21	1.40	0.62	1.45
Healthy values	32.8	6.1	0.18	1.77	0.45	-1.88
Osteoporotic values	9.6	3.8	0.13	0.71	0.87	4.20

BV/TV: bone volume fraction, BS/TV: bone surface fraction, Tb.Th: trabecular thickness, Tb.N: trabecular number, Tb.Sp: trabecular spacing, Tb.Pf: trabecular pattern factor.
Data derived from healthy and osteoporotic bones found in the literature (Chappard, 2012) are displayed in the last lines. Highlighted are parameters of samples from patients undergoing surgery for femoral neck fractures that are comparable to that of osteoporotic bone.

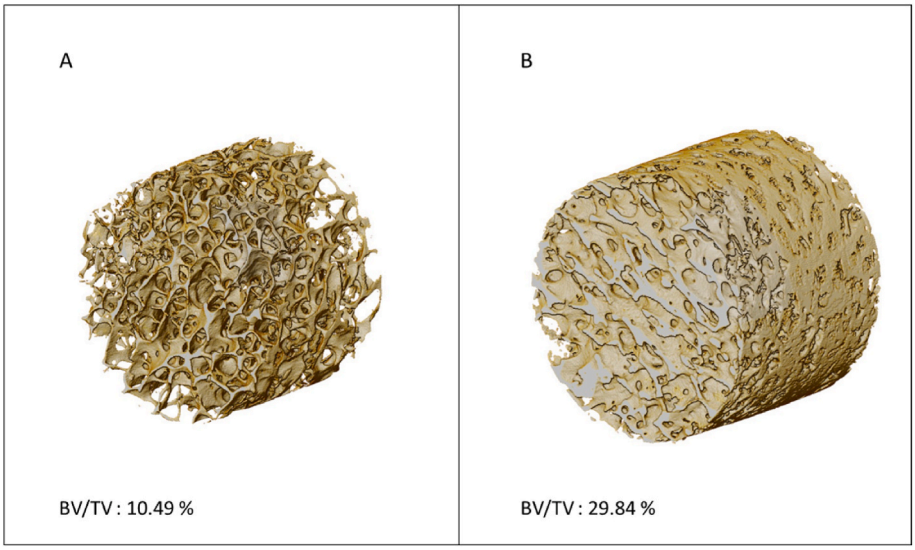

Fig. 6. 3D reconstruction of micro-CT data
Three dimensional µCT reconstruction images of bone biopsies from A. A female patient, aged 92, undergoing surgery for a femoral neck fracture. B. A male patient, aged 52, undergoing surgery for osteoarthritis.
BV/TV: percentage of bone volume on total volume.

phenomenon, it has becoming increasingly clear that a single pathway cannot explain this change in fate and that multiple pathways, mediated by several secreted factors, act in concert (Salmi et al., 2022). The assessment of such complex biological processes couldn't be achieved using conventional functional tests and requires the support of innovative approaches. The use of functional live cell imaging with custom genetically-encoded biosensors and actuators will allow the analysis of intracellular processes in a spatiotemporal way.

CRediT authorship contribution statement

Federica Quacquarelli: Writing – review & editing, Visualization, Validation, Methodology, Investigation, Conceptualization. **Damien Leterme:** Methodology, Investigation, Conceptualization. **Véronique Gauthier:** Methodology, Investigation. **Jérôme Delattre:** Writing – review & editing, Validation, Methodology, Investigation, Formal analysis. **Paiva dos Santos Bruno:** Writing – review & editing, Visualization, Validation, Methodology, Investigation. **Emeline Cailliau:** Writing – review & editing, Formal analysis. **Eric Fodzo:**

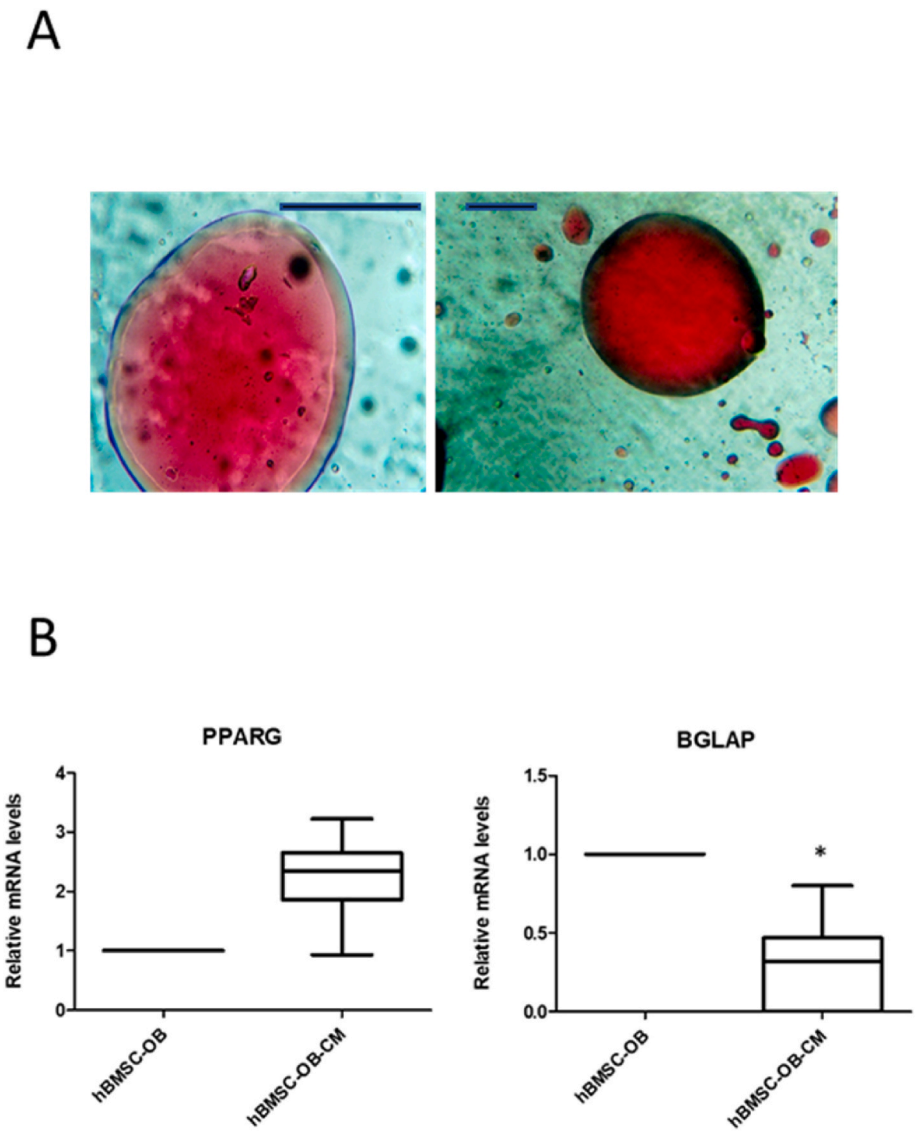

Fig. 7. Primary adipocyte isolation and use of their secretome A. Representative images of primary bone marrow adipocytes stained with Oil red O and counter-stained with hematoxylin after two days in ceiling culture. The adipocytes present a large unilocular cytoplasmic droplet and a small flattened nucleus. Bar = 50 μm. B. Quantitative RT-PCR analysis of adipocyte-specific gene, PPARG (Peroxisome proliferator-activated receptor gamma), and osteoblast-specific gene BGLAP (Bone Gamma-Carboxyglutamate Protein). hBMSC-OB: hBMSC-derived osteoblasts in serum free medium for 48 h hBMSC-OB-CM: hBMSC-OB incubated for 48h in conditioned medium provided by primary adipocytes. mRNA expression levels were normalized to hBMSC-OB expression against the signal from two housekeeping genes for peptidylprolyl isomerase A (PPIA) and tyrosine 3-monooxygenase/tryptophan 5-monooxygenase activation protein (YWHAZ). Results are presented as the median and 1st and 3rd quartile. N = 7 for each group. *P < 0.05, for hBMSC-OB-CM compared to hBMSC-OB.

Resources. **Antonella Poloni:** Resources, Methodology. **Aline Clabaut:** Writing – review & editing, Visualization, Methodology, Investigation, Conceptualization. **Odile Broux:** Writing – original draft, Visualization, Validation, Supervision, Project administration, Methodology, Investigation, Conceptualization.

Acknowledgments

We would like to thank all the surgical teams at Boulogne-sur-Mer Hospital for their invaluable assistance with sample collection, as well as the clinical research team at Ospedale di Ancona, led by Dr. Raffaele Pascarella, for their kind support and collaboration. FQ was supported by a fellowship from UFI (Université Franco Italienne).

Appendix A. Supplementary data

Supplementary data to this article can be found online at https://doi.org/10.1016/j.diff.2026.100947.

References

Chappard, C., 2012. Méthodes d'évaluation de la microarchitecture de l'os trabéculaire humain [Microarchitecture assessment of human trabecular bone: description of methods]. Med. Sci. 28 (12), 1111–1115. https://doi.org/10.1051/medsci/20122812022.

Chen, H., Zhou, X., Fujita, H., Onozuka, M., Kubo, K.Y., 2013. Age-related changes in trabecular and cortical bone microstructure. Int. J. Endocrinol. 2013, 213234. https://doi.org/10.1155/2013/213234.

Clabaut, A., Delplace, S., Chauveau, C., Hardouin, P., Broux, O., 2010. Human osteoblasts derived from mesenchymal stem cells express adipogenic markers upon coculture with bone marrow adipocytes. Differentiation 80 (1), 40–45. https://doi.org/10.1016/j.diff.2010.04.004.

Clabaut, A., Grare, C., Léger, T., Hardouin, P., Broux, O., 2015. Variations of secretome profiles according to conditioned medium preparation: the example of human mesenchymal stem cell-derived adipocytes. Electrophoresis 36 (20), 2587–2593. https://doi.org/10.1002/elps.201500086.

Clabaut, A., Grare, C., Rolland-Valognes, G., Letarouilly, J.G., Bourrier, C., Andersen, T. L., Sikjær, T., Rejnmark, L., Ejersted, C., Pastoureau, P., Hardouin, P., Sabatini, M.,

Broux, O., 2021. Adipocyte-induced transdifferentiation of osteoblasts and its potential role in age-related bone loss. PLoS One 16 (1), e0245014. https://doi.org/10.1371/journal.pone.0245014.

Dillon, J.P., Waring-Green, V.J., Taylor, A.M., Wilson, P.J., Birch, M., Gartland, A., Gallagher, J.A., 2012. Primary human osteoblast cultures. Methods Mol. Biol. 816, 3–18. https://doi.org/10.1007/978-1-61779-415-5_1.

Effendy, N.M., Khamis, M.F., Shuid, A.N., 2013. Micro-CT assessments of potential anti-osteoporotic agents. Curr. Drug Targets 13, 1542–1551. https://doi.org/10.2174/13894501113149990196.

Gartland, A., Rumney, R.M., Dillon, J.P., Gallagher, J.A., 2012. Isolation and culture of human osteoblasts. Methods Mol. Biol. 806, 337–355. https://doi.org/10.1007/978-1-61779-367-7_22.

Geusens, P.P., van den Bergh, J.P., 2016. Osteoporosis and osteoarthritis: shared mechanisms and epidemiology. Curr. Opin. Rheumatol. 28 (2), 97–103. https://doi.org/10.1097/BOR.0000000000000256.

Hardouin, P., Pansini, V., Cortet, B., 2014. Bone marrow fat. Jt. Bone Spine 81 (4), 313–319. https://doi.org/10.1016/j.jbspin.2014.02.013.

Hendijani, F., 2017. Explant culture: an advantageous method for isolation of mesenchymal stem cells from human tissues. Cell Prolif. 50 (2), e12334. https://doi.org/10.1111/cpr.12334.

Laharrague, P., Casteilla, L., 2007. Bone marrow adipose tissue. In: Fantuzzi, G., Mazzone, T. (Eds.), Adipose Tissue and Adipokines in Health and Disease. Nutrition and Health. Humana Press, pp. 159–180. https://doi.org/10.1007/978-1-59745-370-7_13.

Martin, P.J., Haren, N., Ghali, O., Clabaut, A., Chauveau, C., Hardouin, P., Broux, O., 2015. Adipogenic RNAs are transferred in osteoblasts via bone marrow adipocytes-derived extracellular vesicles (EVs). BMC Cell Biol. 16, 10. https://doi.org/10.1186/s12860-015-0057-5.

Mattiucci, D., Maurizi, G., Izzi, V., Cenci, L., Ciarlantini, M., Mancini, S., Mensà, E., Pascarella, R., Vivarelli, M., Olivieri, A., Leoni, P., Poloni, A., 2018. Bone marrow adipocytes support hematopoietic stem cell survival. J. Cell. Physiol. 233 (2), 1500–1511. https://doi.org/10.1002/jcp.26037.

Merrell, A.J., Stanger, B.Z., 2016. Adult cell plasticity in vivo: de-differentiation and transdifferentiation are back in style. Nat. Rev. Mol. Cell Biol. 17 (7), 413–425. https://doi.org/10.1038/nrm.2016.24.

Meunier, P., Aaron, J., Edouard, C., Vignon, G., 1971. Osteoporosis and the replacement of cell populations of the marrow by adipose tissue. A quantitative study of 84 iliac bone biopsies. Clin. Orthop. Relat. Res. 80, 147–154. https://doi.org/10.1097/00003086-197110000-00021.

Muruganandan, S., Govindarajan, R., Sinal, C.J., 2018. Bone marrow adipose tissue and skeletal health. Curr. Osteoporos. Rep. 16 (4), 434–442. https://doi.org/10.1007/s11914-018-0451-y.

Nuttall, M.E., Patton, A.J., Olivera, D.L., Nadeau, D.P., Gowen, M., 1998. Human trabecular bone cells are able to express both osteoblastic and adipocytic phenotype: implications for osteopenic disorders. J. Bone Miner. Res. 13 (3), 371–382. https://doi.org/10.1359/jbmr.1998.13.3.371.

Poloni, A., Maurizi, G., Mattiucci, D., Busilacchi, E., Mancini, S., Discepoli, G., Amici, A., Falconi, M., Cinti, S., Leoni, P., 2015. Biosafety evidence for human dedifferentiated adipocytes. J. Cell. Physiol. 230 (7), 1525–1533. https://doi.org/10.1002/jcp.24898.

Ravazzano, L., Colaianni, G., Tarakanova, A., Xiao, Y.B., Grano, M., Libonati, F., 2024. Multiscale and multidisciplinary analysis of aging processes in bone. NPJ Aging 10 (1), 28. https://doi.org/10.1038/s41514-024-00156-2.

Rizou, S., Chronopoulos, E., Ballas, M., Lyritis, G., 2018. Clinical manifestations of osteoarthritis in osteoporotic and osteopenic postmenopausal women. J. Musculoskelet. Neuronal Interact. 18, 208–214.

Rosen, C.J., Bouxsein, M.L., 2006. Mechanisms of disease: is osteoporosis the obesity of bone? Nat. Clin. Pract. Rheumatol. 2 (1), 35–43. https://doi.org/10.1038/ncprheum0070.

Sadie-Van Gijsen, H., Crowther, N.J., Hough, F.S., Ferris, W.F., 2013. The interrelationship between bone and fat: from cellular see-saw to endocrine reciprocity. Cell. Mol. Life Sci. 70 (13), 2331–2349. https://doi.org/10.1007/s00018-012-1211-2.

Salmi, A., Quacquarelli, F., Chauveau, C., Clabaut, A., Broux, O., 2022. An integrative bioinformatics approach to decipher adipocyte-induced transdifferentiation of osteoblast. Genomics 114 (4), 110422. https://doi.org/10.1016/j.ygeno.2022.110422.

Schilling, T., Nöth, U., Klein-Hitpass, L., Jakob, F., Schütze, N., 2007. Plasticity in adipogenesis and osteogenesis of human mesenchymal stem cells. Mol. Cell. Endocrinol. 271 (1-2), 1–17. https://doi.org/10.1016/j.mce.2007.03.004.

Shah, M., Gburcik, V., Reilly, P., Sankey, R.A., Emery, R.J., Clarkin, C.E., Pitsillides, A.A., 2015. Local origins impart conserved bone type-related differences in human osteoblast behaviour. Eur. Cell. Mater. 29, 155–175. https://doi.org/10.22203/ecm.v029a12.

Song, L., Tuan, R.S., 2004. Transdifferentiation potential of human mesenchymal stem cells derived from bone marrow. FASEB J. 18 (9), 980–982. https://doi.org/10.1096/fj.03-1100fje.

Zhang, C., Li, L., Jiang, Y., Wang, C., Geng, B., Wang, Y., Chen, J., Liu, F., Qiu, P., Zhai, G., Chen, P., Quan, R., Wang, J., 2018. Space microgravity drives transdifferentiation of human bone marrow-derived mesenchymal stem cells from osteogenesis to adipogenesis. FASEB J. 32 (8), 4444–4458. https://doi.org/10.1096/fj.201700208RR.